J. Chem. Thermodynamics 158 (2021) 106423

Contents lists available at ScienceDirect

J. Chem. Thermodynamics

journal homepage: www.elsevier.com/locate/jct

Permittivity of (40 nm and 80 nm) alumina nanofluids in ethylene glycol at different temperatures

M.F. Coelho [a,b], M.A. Rivas [c], E.M. Nogueira [a,b], T.P. Iglesias [c,*]

[a] Departamento de Física-Politécnico do Porto, Instituto Superior de Engenharia, Portugal
[b] CIETI-Centro de Inovação em Engenharia e Tecnologia Industrial, ISEP, Porto, Portugal
[c] Departamento de Física Aplicada, Facultad de Ciencias, Universidad de Vigo, Lagoas-Marcosende s/n, 36310 Vigo, Spain

ARTICLE INFO

Article history:
Received 26 November 2020
Received in revised form 9 February 2021
Accepted 11 February 2021
Available online 13 February 2021

Keywords:
Alumina
Nanofluids
Nanoparticles
Relative permittivity
Theoretical models

ABSTRACT

This article studies the effective permittivity of alumina nanofluids (aluminium oxide) in ethylene glycol. Two nanoparticle sizes (40 nm and 80 nm) were considered and the measurements were carried out at various concentrations (up to 2% in volume) and at six different temperatures (from 298.15 K to 348.15 K). An empirical equation is proposed that allows to obtain the permittivity value at any concentration or temperature in the studied ranges. The influence of the volume fraction, nanoparticle size and the temperature on relative permittivity is shown. When compared to the previous published values for alumina (40 nm) in water, current results show the influence of the base fluid. The enhancement of permittivity was calculated, and its behaviour was analysed. Smaller sized particles have the highest values of permittivity and enhancement. Theoretical models in the study of permittivity are applied. The poor predictions of classical models are attributed to the positive behaviour of the permittivity change on mixing for these nanofluids. The contributions to permittivity from ethylene glycol and nanoparticles are separated in two distinct terms in the variable index equation. The permittivity change on mixing calculated from this equation points out that the nanoparticles are the main responsible for the unusual permittivity increment in these colloids.

1. Introduction

Nanofluids are among the advanced materials that have already been studied for several decades. They are colloids of nanoparticles dispersed in base fluids. It is well known that, in general, their properties depend on the size, concentration and morphology of nanoparticles, the possible addition of surfactants as well as the chemical nature of the nanoparticles and the base fluid. Many different properties of these colloids have been studied in literature because their study is important from both theoretical and experimental points of view. Among these properties, the thermal conductivity is being extensively studied because, in general, when nanoparticles are added to the base fluid, the nanofluid presents a higher thermal conductivity, K, than that of the base fluid, K_B. That is, the enhancement of thermal conductivity, K / K_B, is bigger than one. Permittivity is another quantity that is being studied. Apart from the importance of this study from a fundamental point of view, Koo and Kleinstreuer [1] have also pointed out the significance of this study for the micro heat-sink performance improvements. Subramaniyan *et al.* [2] present studies of dielectric properties as a function of frequency (104 Hz and 107 Hz) at 293.15 K, of TiO_2 with ethylene glycol, propylene glycol and water-based nanofluids and they reported an increase in dielectric constant for all samples. The largest growth was observed for water-based nanofluids. There are not many studies on permittivity behaviour as a function of temperature, particle volume fraction, particle size and purity of the base fluid. The authors T.P. Iglesias *et al.* [3,4] have shown the behaviour of alumina (15, 40 nm) in water based nanofluids at 1 MHz.

In this paper, we will study the permittivity behaviour with temperature of alumina nanofluids with nanoparticles sizes of 40 nm and 80 nm and using ethylene glycol as base fluid. The measurements were carried out without the addition of surfactants in order not to mask the effect of the nanoparticles, thus allowing to highlight the importance of the other factors mentioned above on the behaviour of permittivity and enhancement permittivity of the studied nanofluids.

Since both these magnitudes mentioned above, thermal conductivity and permittivity, have a parallelism in their mathematical formulation, we are tentatively comparing their respective experimental behaviours. Regarding the publications in literature

* Corresponding author.
E-mail address: tpigles@uvigo.es (T.P. Iglesias).

https://doi.org/10.1016/j.jct.2021.106423
0021-9614/

about thermal conductivity of alumina nanofluids using ethylene glycol as base fluid, several authors have measured this quantity showing the following enhancement values in function of nanoparticle volume fraction, temperature and particle size: [5] Georgia et *al.* (5%, 298.15 K, 5 nm) <1.06 at 2% nanoparticle volume fraction; [6] Murshed *et al.* (1% to 5%, 288.15 K to 333.15 K, 80 nm), 1.18 at 5% nanoparticle volume fraction and 1.10 at 2%; [7] Barbés *et al.* (1% to 10%, 298.15 K to 338.15 K, 40 - 50 nm), around 1.15 for 5% nanoparticle volume fraction, and greater than 1.30 at 8%, both to 298.15 K. The values of that ratio as a function of temperature and volume fraction show a slight increase for all volume fractions when the temperature increases; [8] Longo and Zilio, (1% to 3%, 273.15 K to 323.15 K, 10 nm) around 1.18 at 2% nanoparticle volume fraction at 20 °C; [9] Beck *et al.* (2/3/4%, 298.15 K, 8 nm to 282 nm) around 1.06 at 2% particle volume fraction and decreases when nanoparticle size decreases (<50 nm); [10] Beck *et al.* (1% to 4%, 301.15 K to 409.15 K, 20 nm), around 1.15 at 4% particle volume fraction; [11] Lee *et al.* (1% to 5%, room temperature , 25 nm), 1.10 at 3% and 1.18 at 5%; [12] Timofeeva *et al.* (0% to 10%, 296.15 K, 40 nm) 1.13 at 5% nanoparticle volume fraction; [13] Pastoriza-Gallego *et al.* (1.5% to 8.6%, 283.15/303.15/323.15 K, 40 - 50 nm) 1.05 at 2% nanoparticle volume fraction at 303.15 K; [14] Patel *et al.* (0.5% to 3%, 293.15 K to 323.15 K, 11/45/150 nm) 1.14 at 2% nanoparticle volume fraction at 323.15 K. From the work of these authors, we will try to find analogies or differences between the behaviours of permittivity and thermal conductivity enhancements of the nanofluids under study.

The paper is organized as follows. In section 2, the experimental details are described. In section 3, the results and the data analysis are presented. In section 4, a summary of the main conclusions is made.

2. Materials and methods

2.1. Materials

The provenance and purity of the materials studied are summarised in Table 1. Alpha-alumina nanoparticles (α-Al_2O_3), with an average particle size of 40 nm, were supplied by MK-nano. The purity of these aluminium oxide nanoparticles was greater than 0.995 mass and a stated density of 3.7 g · cm^{-3}. This value is in good agreement with the density range (3.75 to 3.95) g · cm^{-3} given by Morrell [15] for bulk alumina having 0.2% to 3% porosity. Alpha-alumina nanoparticles (α-Al_2O_3) with an average particle size of 80 nm were supplied by Iolitec. The purity of these aluminium oxide nanoparticles was greater than 0.995 mass and a stated density of 4 g · cm^{-3}. This value is in good agreement with the density range (3.90 to 3.99) g · cm^{-3} given by Morrell [15] for bulk alumina, having a porosity smaller than 1%. Ethylene glycol, EG, was supplied by Sigma Aldrich with a purity greater than 99% (GC). This was degassed ultrasonically, dried over molecular sieves type (3 and 4) 10^{-8} cm supplied by Aldrich and kept in inert argon. As it is hygroscopic after carrying out the measurements, its water mass fraction was determined by Karl Fisher coulometer (Mettler Toledo DL 32). Table 2 compares the permittivity values for the ethylene glycol with those of literature.

Table 1
Specifications for pure components.

Name	Alumina (40 nm)	Alumina (80 nm)	Ethylene glycol
Chemical formula	α-Al_2O_3	α-Al_2O_3	$C_2H_6O_2$
CAS number	1344–28-1	1344–28-1	107–21-1
Supplier	MK-nano	Iolitec	Sigma Aldrich
Mass fraction Purity	greater than 0.995 [a]	greater than 0.995 [a]	greater than 0.99 [a,b]

[a] stated by the supplier.
[b] the measured water content using a Karl Fisher coulometer (Mettler Toledo DL 32) was 980 ppm.

2.2. Preparation of the nanofluids

In order to minimise errors in achieving the nanofluids, the nanoparticles were stored in airtight and opaque vials throughout the process to avoid contact with light and air.

To prepare an alumina nanofluid sample in ethylene glycol at a certain volume fraction, the required amount of nanoparticle mass, which was calculated with the density provided by the manufacturers, was added to a certain amount of mass of base fluid. The alumina volume fraction, ϕ_A, was calculated using the equation (1), [3,4],

$$\phi_A = x_A V_A^* / [(1 - x_A) V_{EG}^* + x_A V_A^*] \quad (1)$$

where x_A and V_A^* stand for the alumina mole fraction and molar volume, respectively. Ethylene glycol molar volume, V_{EG}^*, was obtained from its density, Table S1, which was measured with an Anton Paar DMA-4500 densimeter with a precision of ± 10^{-5} g · cm^{-3}, [23]. Before taking the measurements, this instrument was calibrated with Millipore quality water and ambient air, respectively, in accordance with the instructions.

All samples were prepared using a Mettler balance AE-240, which has a $5 \cdot 10^{-5}$g accuracy and a resolution of $\pm 10^{-4}$ g.

To obtain a uniform dispersion and prevent aggregation of the nanoparticles, the Bandelin Sonoplus HD2200 ultrasonic homogeniser was used. Its 20 kHz oscillations are transmitted and amplified through TT 13 titanium tip, 13 mm in diameter. A similar procedure to that used in [3,4] was followed. The sonication was applied for 60 min at 10% of maximum power. In order to prevent overheating, the sonication was applied in six time intervals of ten minutes, with a three-minute break between them, and the vial containing the sample was immersed in an ice bath throughout the sonication process.

2.3. Measurement of permittivity

The relative permittivity, ε_r, measurements were carried out using a HP4284A precision LCR Meter with a range of frequency of 1 kHz to 1 MHz. This meter was connected to a HP16452A measurement cell, which has parallel plate geometry, through a HP16452-61601 test lead. The equipment is fully automatic and computer-controlled by means of a HP-IB and an average of sixteen values for permittivity was obtained at each experimental frequency. The measurement cell was thermostatted using a PolyScience fluid circulation bath, which controlled the temperature to

Table 2
Comparison between experimental relative permittivity, ε_r, and data in the literature for ethylene glycol at the work temperatures and at the pressure of 96.5kPa[a].

T/K	ε_r	Literature
298.15	40.77	40.82 [16], 40.96 [17], 40.253[18], 41.2 [19], 40.25 [20], 40.35 [21]
308.15	38.62	38.69 [16], 38.89 [22], 38.90 [17], 38.229 [18], 39.2 [19], 38.22 [20]
318.15	36.63	36.69 [16], 36.98 [22], 36.94 [17], 37.5 [19], 36.29 [20]
328.15	34.85	34.82 [16], 35.09 [17], 35.2 [19], 34.45 [20]
338.15	33.14	33. 06 [16], 33.32 [17], 32.70 [20]
348.15	31.63	31.39 [16], 31.65 [17], 31.04 [20]

[a] Standard uncertainties u are $u(T)$ = 0.01 K, $u(p)$ = 0.5 kPa and the combined expanded uncertainties, $U_c(\varepsilon)$ = 1% with 0.95 level of confidence ($k \approx 2$).

within ± 0.01 K. The description of this equipment can be seen elsewhere [24].

In this work, the reported relative permittivity values were obtained at 1 MHz. At this frequency, the reliability of the measurements has been checked [24–26], and an uncertainty of <1% is estimated.

3. Results and discussion

Figure 1 shows the effect of temperature and nanoparticle concentration on the relative permittivity of the alumina (40 nm)-ethylene glycol nanofluid. The numerical values are reported in Table S2. Relative permittivity decreases with increasing temperature and, at fixed temperature, it increases slightly with increasing concentration of nanoparticles. A similar behaviour was obtained for alumina (80 nm) in ethylene glycol nanofluid showing values slightly smaller than those of alumina (40 nm). The numerical values are reported in Table S3. The behaviour of both nanofluids with temperature and concentration of the nanoparticles is similar to those obtained for Al_2O_3 (15 or 40) nm in water nanofluids [3,4]. As the base fluid contributes to thermophysical properties of nanofluids, Fig. 1 also shows the behaviour of the relative permittivity of the ethylene glycol base fluid at the experimental temperatures. It also decreases with rising temperature.

The relative permittivity data for each nanofluid system are accurately described as a function of the alumina volume fraction and temperature by the following double-polynomial expression:

$$\ln \varepsilon_r = \sum_i \sum_j C_{ij} (T/\mathrm{K})^i \cdot \varnothing_A^j \qquad (2)$$

the best-fitting parameters, C_{ij}, are listed in Table 3 together with their corresponding standard deviations, s, calculated according to:

$$s = \left(\frac{\sum_i^N (y_{i,\mathrm{exp}} - y_{i,\mathrm{calc}})^2}{N-k} \right)^{\frac{1}{2}} \qquad (3)$$

where y and N stand for the property values and the number of experimental data, respectively. k represents the number of adjustable parameters used in the expression.

Regarding the permittivity enhancement, $\varepsilon_r/\varepsilon_{r,EG}$, and analysing the graphs in Fig. 2 it is possible to see that the permittivity enhancement increases with the concentration of nanoparticles and temperature, and this effect is smaller the larger the size of the nanoparticles.

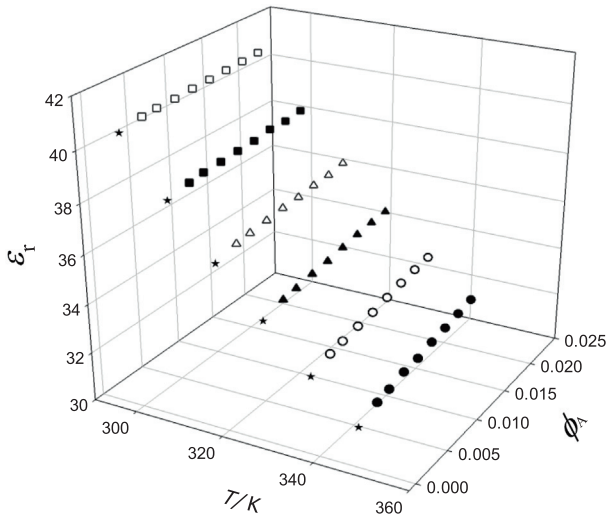

Fig. 1. Experimental relative permittivity, ε_r, of the nanofluid α-Al_2O_3 (40 nm) + ethylene glycol as a function of alumina volume fraction, ϕ_A, and temperature, T: □, T = 298.15 K; ■, T = 308.15 K; △, T = 318.15 K; ▲, T = 328.15 K; ○, T = 338.15 K; ●, T = 348.15 K. Stars stand for relative permittivity of ethylene glycol.

Fig. 2 shows that, for each temperature, the permittivity enhancement is slightly higher than that of the base fluid for all concentrations of alumina nanoparticles. The relative permittivity of solid alumina is rather insensitive to temperature variation in the experimental range [15], and values for $\varepsilon_{r,A}$ between 9 and 10.5 can be found in literature [15,27–29]. Note that, since the relative permittivity of alumina is lower than that of the ethylene glycol, $\varepsilon_{r,EG.}$, the permittivity of the nanofluid should be lower than the source fluid, which does not happen.

To the best of our knowledge, in literature, there are no known studies for these nanofluids that relate the permittivity of the nanofluid, ε_r, to the permittivity of the base fluid, $\varepsilon_{r,EG}$. So, we compared the permittivity enhancement to the thermal conductivity enhancement K/K_{EG}, due to the parallelism in the mathematical formulation for these two physical quantities. The numerical values of K/K_{EG} obtained at room temperature by Lee *et al.* [30] for alumina nanoparticles with a mean diameter of 38 nm and those obtained by Pastoriza *et al.* [13] with a diameter of (40–50) nm are of the same order of magnitude as those of $\varepsilon_r/\varepsilon_{r,EG}$ obtained in this study. Regarding this, it seems that the parallelism in the behaviour of K/K_{EG} and $\varepsilon_r/\varepsilon_{r,EG}$ already observed in [4] remains for the alumina (40 nm) + ethylene glycol nanofluid. However, the finding by Pastoriza *et al.* [13] that the K/K_{EG} is nearly independent with rising temperature seems not to be verified for $\varepsilon_r/\varepsilon_{r,EG}$ as shown in Fig. 2. Contrarily, Barbés *et al.* [7] found that the thermal conductivity enhancement for alumina (40–50) nm + ethylene glycol nanofluid increases with temperature and nanoparticles volume fraction present a similar behaviour to that of $\varepsilon_r/\varepsilon_{r,EG}$.

Because the base fluid contributes to the permittivity enhancement, Fig. 3 compares the behaviour of this quantity for α-Al_2O_3 nanofluids (40 nm) in water [4] and in ethylene glycol. This figure shows that the permittivity enhancement is smaller for the nanofluid with ethylene glycol as base fluid.

In order to see the influence of the size of the nanoparticles, the behaviour of this quantity is compared in Fig. 4 for both nanofluids, α-Al_2O_3 (40 nm) or α-Al_2O_3 (80 nm) in ethylene glycol. It seems that $\varepsilon_r/\varepsilon_{r,EG}$ increases when the size of nanoparticles is smaller. The same behaviour was found in the study of the aqueous nanofluids of α-Al_2O_3 (40 nm) and γ-Al_2O_3 (15 nm), [3,4]. Patel *et al.* [14] also found a similar behaviour for the enhancement of thermal conductivity of three different Al_2O_3 + ethylene glycol nanofluids using alumina nanoparticle sizes of 11 or 45 or 150 nm.

The improvement of the permittivity gives a direct estimation of the impact of the nanoparticles in the relative permittivity of the base fluid. However, according to a fundamental standpoint, the relative permittivity of mixing $\Delta_{mix}\varepsilon_r$ is more interesting. For fixed temperature and pressure, this property is defined by the Eq. (4) where $\phi_{EG} = 1 - \phi_A$, ϕ_{EG} represents the volume fraction of ethylene glycol and $\varepsilon_{r,A}$ is the relative permittivity of bulk alumina.

$$\Delta_{mix}\varepsilon_r = \varepsilon_r - (\phi_{EG}\varepsilon_{r,EG} + \phi_A\varepsilon_{r,A}) \qquad (4)$$

For liquid mixtures, the sum within parenthesis is the ideal permittivity [31,32] and, in this case, Eq. (4) is the excess permittivity of the mixture which represents the deviation from the ideal behaviour of the mixture.

In order to illustrate the application of Eq. (4) a temperature independent value of $\varepsilon_{r,A}$ = 9.8 [29] was chosen. The calculated values of $\Delta_{mix}\varepsilon_r$ for alumina (40 nm) in ethylene glycol nanofluid are represented in Fig. 5. For a better visualization, only three temperatures were depicted. Tables S4 and S5 show that the values of $\Delta_{mix}\varepsilon_r$ are positive for all temperatures and concentrations, which means that the polarization is larger in the real mixture in relation

Table 3
Coefficients C_{ij} of Eq. (2) and their standard deviations, s, for the two nanofluids.

Nanofluid	C_{00}	C_{01}	C_{02}	C_{10}	C_{11}	s
α-Al_2O_3 (40 nm) + EG	5.1555	0.0976	0.0331	−0.0049	0.0032	0.004
α-Al_2O_3 (80 nm) + EG	5.1760	0.0976	0.0331	−0.0049	0.0012	0.004

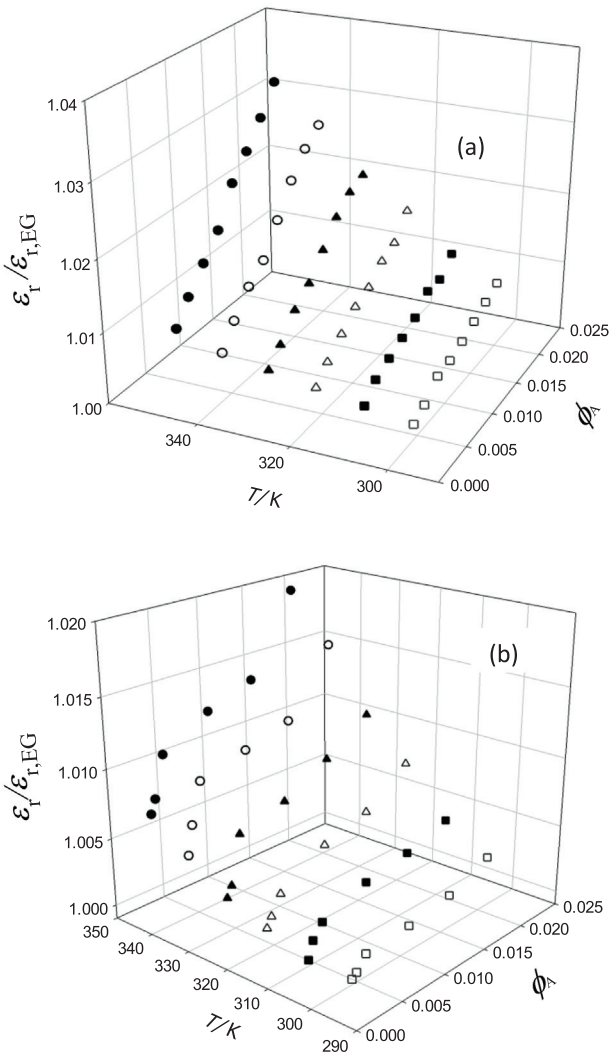

Fig. 2. Permittivity enhancement, $\varepsilon_r/\varepsilon_{r,EG}$, for the nanofluids (a) α-Al_2O_3 (40 nm) + ethylene glycol and (b) α-Al_2O_3 (80 nm) + ethylene glycol as a function of alumina volume fraction, ϕ_A, at different temperatures: □, T = 298.15 K; ■, T = 308.15 K; △, T = 318.15 K;▲, T = 328.15 K;○, T = 338.15 K; ●, T = 348.15 K.

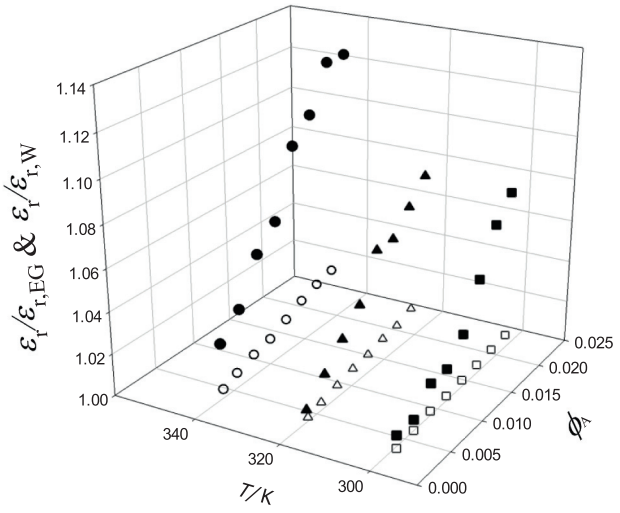

Fig. 3. Permittivity enhancements, $\varepsilon_r/\varepsilon_{r,EG}$ and $\varepsilon_r/\varepsilon_{r,W}$ for the nanofluids α-Al_2O_3 (40 nm) + ethylene glycol (open symbols) and α-Al_2O_3 (40 nm) + Milli-Q water (filled symbols) [4] as a function of alumina volume fraction, ϕ_A, at three different temperatures: squares, T = 298.15 K; triangles, T = 318.15 K; circles, T = 338.15 K.

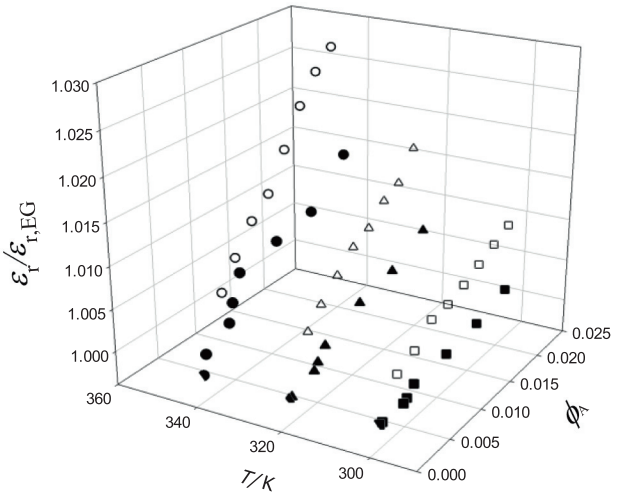

Fig. 4. Permittivity enhancements, $\varepsilon_r/\varepsilon_{r,EG}$ for the nanofluids α-Al_2O_3 (40 nm) + ethylene glycol (open symbols) and α-Al_2O_3 (80 nm) + ethylene glycol (filled symbols) as a function of alumina volume fraction, ϕ_A, at three different temperatures: squares, T = 298.15 K; triangles, T = 318.15 K; circles, T = 338.15 K.

to that of the ideal one. This behaviour is in line with the temperature dependency of the permittivity enhancement shown in Fig. 2. Fig. 5 shows that $\Delta_{mix}\varepsilon_r$ increases with increasing temperature, which is an unusual behaviour when compared to that of the excess permittivity of the binary liquid mixtures. This last quantity, in general, tends to decrease with rising temperature [24,33,34]. In other words, the binary liquid systems approach ideal behaviour when temperature increases. A positive behaviour of $\Delta_{mix}\varepsilon_r$ that moves away from ideal behaviour when rising temperature was also observed for the aqueous alumina nanofluids [3,4].

In order to separate the contributions to ε_r, of each of the two components of the nanofluid, the empirical equation (5) of variable index is considered

$$\varepsilon_r = \varnothing_{EG} \cdot \varepsilon^I_{r,EG} + \varnothing_A \cdot \varepsilon^J_{r,A} \quad (5)$$

where I and J are empirical fitting parameters. A similar equation was proposed in [35] to separate the contributions to the electrical conductivity from the nanoparticles and the base fluid.

Table 4 shows the values of I and J at the different temperatures. The values of I are close to one for all temperatures.

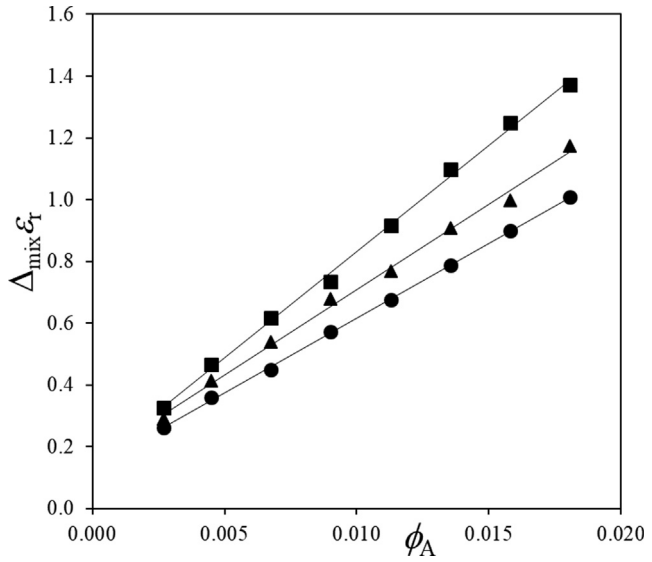

Fig. 5. Relative permittivity of mixing, $\Delta_{mix}\varepsilon_r$, for de system α-$Al_2O_3$ (40 nm) + ethylene glycol as a function of alumina volume fraction, ϕ_A, at three different temperatures: ●, T = 298.15 K; ▲, T = 318.15 K and ■, T = 338.15 K. Continuous lines are drawn as eye-guides.

By Eq. (5) the separation of the two contributions to permittivity of mixing can be obtained:

$$\Delta_{mix}\varepsilon_r = \varnothing_{EG}\cdot(\varepsilon^I_{EG} - \varepsilon_{EG}) + \varnothing_{r,A}\cdot(\varepsilon^J_A - \varepsilon_A) = \Delta_{mix}\varepsilon_{r,EG} + \Delta_{mix}\varepsilon_{r,A} \quad (6)$$

In this equation, $\Delta_{mix}\varepsilon_{r,EG}$ and $\Delta_{mix}\varepsilon_{r,A}$ represent the contribution of ethyleneglycol and that of alumina to permittivity change on mixing, respectively.

In Fig. 6, the two contributions to ε_r are shown for alumina {(80 nm) + ethylene glycol} nanofluid. A similar behaviour is obtained for alumina {(40 nm) + ethylene glycol} nanofluid. It can be seen that the contribution of the base fluid is much higher than that of the nanoparticles. However, Fig. 7, where the two contributions $\Delta_{mix}\varepsilon_{r,EG}$ and $\Delta_{mix}\varepsilon_{r,A}$ from Eq. (6) are represented separately, shows that the contribution of the alumina nanoparticles,$\Delta_{mix}\varepsilon_{r,A}$, is higher than that of the base fluid,$\Delta_{mix}\varepsilon_{r,A} > \Delta_{mix}\varepsilon_{r,EG}$. That is, as the base fluid has a permittivity higher than that of the alumina bulk its contribution to ε_r is the highest, Fig. 6. However, Fig. 7 shows that the alumina nanoparticles are the main responsible for the deviation from the ideal behaviour and, therefore, the main responsible for the unusual increment of the permittivity of these colloids.

For both nanofluids, the behaviours of $\Delta_{mix}\varepsilon_{r,A}$ and $\Delta_{mix}\varepsilon_{r,EG}$ with the nanoparticle concentration are similar, Fig. 7. $\Delta_{mix}\varepsilon_{r,A}$increases linearly while $\Delta_{mix}\varepsilon_{r,EG}$is nearly constant. However, their behaviours with temperature are opposite. For the nanofluid of alumina (40 nm) $\Delta_{mix}\varepsilon_{r,A}$increases with temperature while $\Delta_{mix}\varepsilon_{r,EG}$ presents a very small dependence on this quantity, Fig. 7a. For the nanofluid

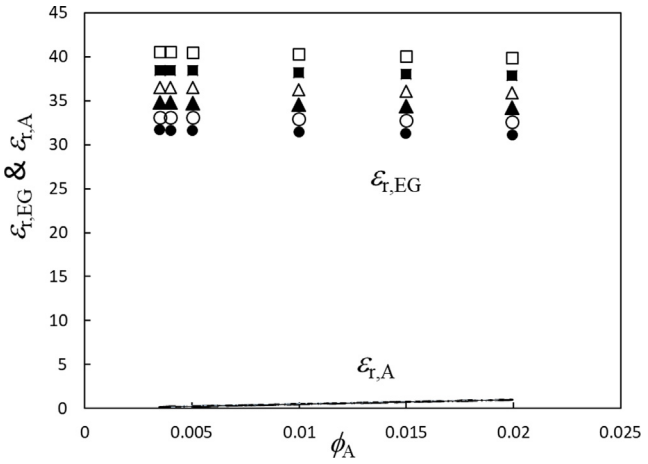

Fig. 6. Contributions to the permittivity, Eq. (5), from the base fluid, $\varepsilon_{r,EG}$and from nanoparticles, $\varepsilon_{r,A}$, as a function of alumina volume fraction, ϕ_A, and temperature, T, for the alumina (80 nm) + EG nanofluid. Symbols: □, T = 298.15; ■, T = 308.15; △, T = 318.15; ▲, T = 328.15; ○, T = 338.15; ●, T = 348.15 K. The continuous line represents the behaviour of $\varepsilon_{r,A}$ at all those temperatures.

of alumina (80 nm) the change with temperature of $\Delta_{mix}\varepsilon_{r,A}$is very small while $\Delta_{mix}\varepsilon_{r,EG}$ slowly increases with temperature, Fig. 7b.

We have compared our experimental permittivity data with those predicted by some theoretical models for binary mixtures. Among those that offered the best results for the standard deviation, see Eq. (3), we present in Table 5 the outcome of three that we have considered the more representative. The Looyenga's model [36], Eq. (7), and the Maxwell model [37], also known as Maxwell-Garnett, Eq. (8). They are representing the classical models.

$$\varepsilon_r = \left[\varepsilon^{1/3}_{r,EG} + \varnothing_A\left(\varepsilon^{1/3}_{r,A} - \varepsilon^{1/3}_{r,EG}\right)\right]^3 \quad (7)$$

$$\varepsilon_r = \varepsilon_{r,EG}\left[\frac{\varepsilon_{r,A} + 2\varepsilon_{r,EG} + 2(\varepsilon_{r,A} - \varepsilon_{r,EG})\varnothing_A}{\varepsilon_{r,A} + 2\varepsilon_{r,EG} - (\varepsilon_{r,A} - \varepsilon_{r,EG})\varnothing_A}\right] \quad (8)$$

The third theoretical model considered represents the models that were specifically formulated for nanofluids without any coefficient of fitting in its deduction. Attending to the parallelism in the mathematical formulation for permittivity and thermal conductivity, we have adapted the equation from the Nan *et al.* [38] developed for thermal conductivity of carbon nanotubes nanofluids to our relative permittivity data in the following form,

$$\varepsilon_r = \frac{3 + \phi_A(\varepsilon_{r,A}/\varepsilon_{r,EG})}{3 - 2\phi_A}\varepsilon_{r,EG} \quad (9)$$

Table 5 shows the good ability of this model to predict the experimental values even though the size of the nanoparticles is not specifically considered in Eq. (9). Attending the values of the standard deviation, its prediction is much better than those from

Table 4
Coefficients I, J of Eq. (5) and the standard deviation, s, for the two nanofluids.

	α-Al_2O_3 (40 nm)			α-Al_2O_3 (80 nm)		
T/K	I	J	s	I	J	s
298.15	1.0009	1.7822	0.01	0.9995	1.7230	0.06
308.15	1.0011	1.7939	0.02	0.9999	1.7094	0.02
318.15	1.0012	1.8322	0.02	1.0001	1.7239	0.02
328.15	1.0012	1.8789	0.02	1.0004	1.7383	0.04
338.15	1.0012	1.9170	0.02	1.0012	1.7233	0.04
348.15	1.0018	1.9218	0.02	1.0014	1.7360	0.04

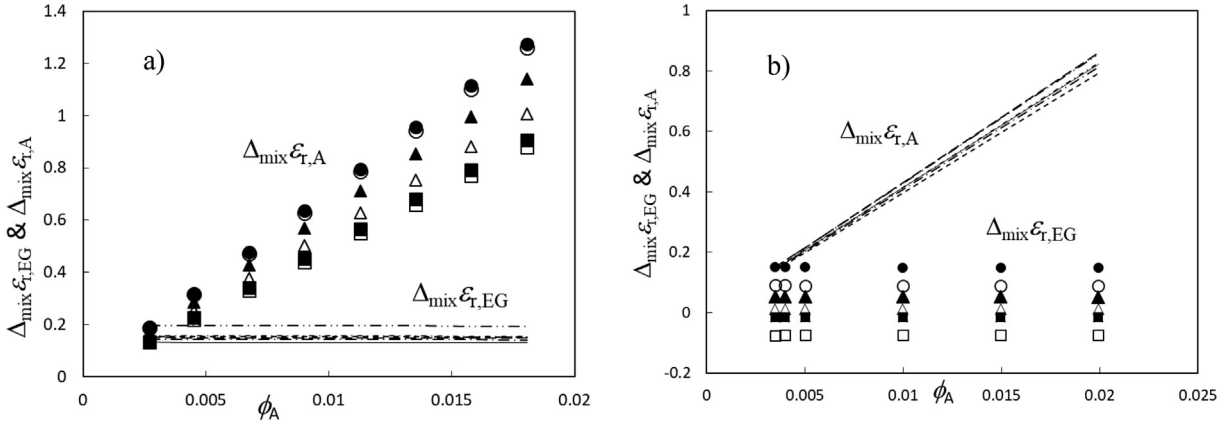

Fig. 7. Contributions to the permittivity of mixing from the base fluid, $\Delta_{mix}\varepsilon_{r,EG}$ and from nanoparticles, $\Delta_{mix}\varepsilon_{r,A}$ as a function of alumina volume fraction, ϕ_A, and temperature, *T*. Symbols: ___, □, 298.15; - - - -, ■ , 308.15; - · - · -, △, 318.15; __ __ __, ▲, 328.15; __.__.__, ○, 338.15; __ .. __ .. ●, 348.15 K. a) alumina (40 nm) + EG; b) alumina (80 nm) + EG.

Table 5
Comparison of predictive ability of different theoretical models for the relative permittivity of present nanofluid systems measured by the standard deviation calculated using Eq. (3).

Theoretical model	α-Al_2O_3 (40 nm)	α-Al_2O_3 (80 nm)
	ethylene glycol	
Looyenga, equation (7)	0.95	0.86
Maxwell, equation (8)	0.91	0.83
Nan *et al*., equation (9)	0.24	0.16

the classical models of Looyenga and Maxwell. However, this equation does not predict adequately the experimental behaviour, as we will see below.

Although the calculated standard deviation of the experimental data with respect to theoretical values is the same for ε_r and $\Delta_{mix}\varepsilon_r$ this latter allows a better visualization of the deviations of theoretical values with respect to the experimental ones. While the classical models predict a behaviour of $\Delta_{mix}\varepsilon_r < 0$, Eq. (9) predicts its positive behaviour correctly, see Tables S4, S5, S6 and S7. Furthermore, the experimental values of $\Delta_{mix}\varepsilon_r$ deviate from the ideal behaviour when temperature increases while their predicted values from Eq. (9) follow the opposite behaviour and close to the ideal behaviour, see Fig. 8. As in the case of alumina (15 or 40 nm) + water nanofluids [3,4], the models that were formulated for nanofluids have performed better than the classical ones.

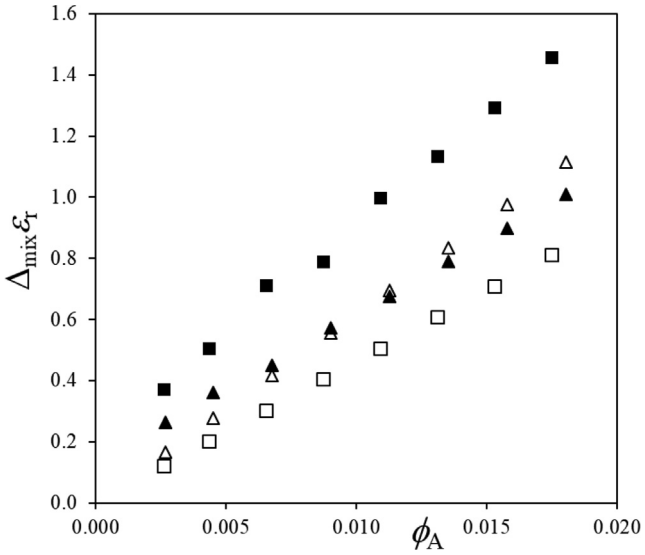

Fig. 8. Relative permittivity of mixing, $\Delta_{mix}\varepsilon_r$, for the system α-Al_2O_3 (40 nm) + ethylene glycol as a function of alumina volume fraction, ϕ_A at two different temperatures: T = 298.15 K are represented by triangles and T = 348.15 K by squares. Experimental values are represented by filled symbols and the theoretical ones using equation (9) by open symbols.

4. Conclusions

From the experimental determination of relative permittivity of nanofluids constituted by alumina particles of different sizes, 40 nm and 80 nm, in base ethylene glycol having concentrations up to a volume fraction of 2% in the temperature range (298–348) K, we draw the following conclusions.

The relative permittivity decreases with increasing temperature and increases with increasing concentration. The permittivity enhancement ($\varepsilon_r/\varepsilon_{r,EG}$) increases while increasing both temperature and concentration. This enhancement is more pronounced in the nanofluid with nanoparticles of smaller size (40 nm). This could be because of the definition of nanofluid; that is, as the size of the nanoparticles approaches 100 nm the special properties of the nanofluids will gradually disappear. Keeping the nanoparticle size, the nanofluids with water as base fluid have larger permittivity enhancement than those that have the ethylene glycol. Similar behaviours were found in literature for the enhancement of thermal conductivity.

The observed positive deviations of the relative permittivity in relation to its ideal value ($\Delta_{mix}\varepsilon_r > 0$) indicate that the polarization of real nanofluids is larger than would be expected. This positive behaviour may explain why classical equations for prediction of permittivity failed when they were applied to the present nanofluids. Indeed, these classic models lead to $\Delta_{mix}\varepsilon_r < 0$.

The Eq. (5) of variable index predicts that the base fluid has a higher contribution to the permittivity of the nanofluid than that of the alumina nanoparticles. However, the permittivity of mixing values from Eq. (6) point out that the nanoparticles are the main responsible of the unusual permittivity increment in these colloids.

CRediT authorship contribution statement

M.F. Coelho: Investigation, Writing-review & editing. **M.A. Rivas:** Data curation, Formal analysis. **E.M. Nogueira:** Investigation, Writing-review & editing. **T.P. Iglesias:** Data curation, Formal analysis, Writing-original draft.

Declaration of Competing Interest

The authors declare that they have no known competing financial interests or personal relationships that could have appeared to influence the work reported in this paper.

Acknowledgements

We appreciate the financial support ED431C 2020-06 provided by the Xunta de Galicia (Spain). M.F.C. thanks Instituto Superior de Engenharia do Porto for granting leave of absence to carry out experimental work at University of Vigo.

Appendix A. Supplementary data

Supplementary data to this article can be found online at https://doi.org/10.1016/j.jct.2021.106423.

References

[1] J. Koo, C. Kleinstreuer, A new thermal conductivity model for nanofluids, J. Nanopart. Res. 6 (2004) 577–588, https://doi.org/10.1007/s11051-004-3170-5.
[2] A. Subramaniyan, L.P. Sukumaran, R. Ilangovan, Investigation of the dielectric properties of TiO 2 nanofluids, J. Taibah Univ. Sci. 10 (2016) 403–406, https://doi.org/10.1016/j.jtusci.2015.05.005.
[3] T.P. Iglesias, M.A. Rivas, R. Iglesias, J.C.R. Reis, F. Cohelho, Electric permittivity and conductivity of nanofluids consisting of 15nm particles of alumina in base Milli-Q and Milli-Ro water at different temperatures, J. Chem. Thermodyn. 66 (2013) 123–130, https://doi.org/10.1016/j.jct.2013.06.019.
[4] R. Iglesias, M.A. Rivas, J.C.R. Reis, T.P. Iglesias, Permittivity and electric conductivity of aqueous alumina (40nm) nanofluids at different temperatures, J. Chem. Thermodyn. 89 (2015) 189–196, https://doi.org/10.1016/j.jct.2015.05.021.
[5] G.J. Tertsinidou, C.M. Tsolakidou, M. Pantzali, M.J. Assael, L. Colla, L. Fedele, S. Bobbo, W.A. Wakeham, New measurements of the apparent thermal conductivity of nanofluids and investigation of their heat transfer capabilities, J. Chem. Eng. Data 62 (2017) 491–507, https://doi.org/10.1021/acs.jced.6b00767.
[6] S.M.S. Murshed, Simultaneous measurement of thermal conductivity, thermal diffusivity, and specific heat of nanofluids, Heat Transfer Eng. 33 (2012) 722–731, https://doi.org/10.1080/01457632.2011.635986.
[7] B. Barbés, R. Paramo, E. Blanco, M.J. Pastoriza-Gallego, M.M. Pineiro, J.L. Legido, C. Casanova, Thermal conductivity and specific heat capacity measurements of Al_2O_3 nanofluids, J. Therm. Anal. Calorim. 111 (2013) 1615–1625, https://doi.org/10.1007/s10973-012-2534-9.
[8] G.A. Longo, C. Zilio, Experimental measurements of thermophysical properties of Al_2O_3- and TiO2−ethylene glycol nanofluids, Int. J. Thermophys. 34 (2013) 1288–1307, https://doi.org/10.1007/s10765-013-1478-z.
[9] M.P. Beck, Y. Yuan, P. Warrier, A.S. Teja, The effect of particle size on the thermal conductivity of alumina nanofluids, J. Nanopart. Res. 11 (2009) 1129–1136, https://doi.org/10.1007/s11051-008-9500-2.
[10] M.P. Beck, Y. Yuan, P. Warrier, A. Teja, The thermal conductivity of alumina nanofluids in water, ethylene glycol, and ethylene glycol + water mixtures, J. Nanopart. Res. 12 (2010) 1469–1477, https://doi.org/10.1007/s11051-009-9716-9.
[11] S. Lee, S.U.-S. Choi, S. Li, J.A. Eastman, Measuring thermal conductivity of fluids containing oxide nanoparticles, J. Heat Transfer 121 (1999) 280–289, https://doi.org/10.1115/1.2825978.
[12] E.V. Timofeeva, A.N. Gavrilov, J.M. McCloskey, Y.V. Tolmachev, S. Sprunt, L.M. Lopatina, J.V. Selinger, Thermal conductivity and particle agglomeration in alumina nanofluids: Experiment and theory, Phys. Rev. E 76 (2007), https://doi.org/10.1103/PhysRevE.76.061203 061203.
[13] M.J. Pastoriza-Gallego, L. Lugo, J.L. Legido, M.M. Piñeiro, Thermal conductivity and viscosity measurements of ethylene glycol based Al_2O_3 nanofluids, Nanoscale Res. Lett. 6 (2011) 221–231, https://doi.org/10.1186/1556-276X-6-221.
[14] H.E. Patel, T. Sundararajan, S.K. Das, An experimental investigation into the thermal conductivity enhancement in oxide and metallic nanofluids, J. Nanopart. Res. 12 (2010) 1015–1031, https://doi.org/10.1007/s11051-009-9658-2.
[15] R. Morrell, Handbook of Properties of Technical and Engineering Ceramics, Part 2, Section I, High-alumina Ceramics, Her Majesty's Stationary Office, London, 1987.
[16] N.V. Lifanova, T.M. Usacheva, M.V. Zhuravlev, Equilibrium and relaxation dielectric properties of 1,2-ethanediol, Russ. J. Phys. Chem. A 81 (2007) 820–828, https://doi.org/10.1134/S0036024407050305.
[17] R. Nagarajan, Chien-Chung Wang, Theory of surfactant aggregation in water/ethylene glycol mixed solvents, Langmuir 16 (2000) 5242–5251, https://doi.org/10.1021/la9910780.
[18] N.V. Sastry, M.C. Patel, Densities, excess molar volumes, viscosities, speeds of sound, excess isentropic compressibilities, and relative permittivities for alkyl (Methyl, Ethyl, Butyl, and Isoamyl) acetates + glycols at different temperatures, J. Chem. Eng. Data 48 (2003) 1019–1027, https://doi.org/10.1021/je0340248.
[19] R.J. Sengwa, A comparative dielectric study of ethylene glycol and propylene glycol at different temperatures, J. Mol. Liq. 108 (2003) 47–60, https://doi.org/10.1016/S0167-7322(03)00173-9.
[20] D.R. Lide (Ed.), Handbook of Chemistry and Physics, 87 ed., 2007.
[21] Cezary M. Kinart, Magdalena Klimczak, Wojciech J. Kinart, Volumetric and dielectric characterization and analysis of internal structure of binary mixtures of 2-ethoxyethanol with ethylene glycol, diethylene glycol, triethylene glycol, and tetraethylene glycol at T = (293.15, 298.15 and 303.15) K, J. Mol. Liq. 145 (2009) 8–13. 10.1016/j.molliq.2008.11.002.
[22] F. Corradini, M. Malagoli, L. Marcheselli, A. Marchetti, L. Tassi, Dielectric properties of ethane-1,2-diol + 2-methoxyethanol + water liquid ternary mixtures, J. Chem. Eng. Data 38 (1993) 565–568, https://doi.org/10.1021/je00012a022.
[23] J.N. Real, T.P. Iglesias, S.M. Pereira, M.A. Rivas, Analysis of temperature dependence of some physical properties of (n-nonane + tetraethylene glycol dimethyl ether), J. Chem. Thermodyn. 34 (2002) 1029–1043, https://doi.org/10.1006/jcht.2002.0981.
[24] T.P. Iglesias, J.L. Legido, S.M. Pereira, B.E. de Cominges, M.I. Paz Andrade, Relative permittivities and refractive indices on mixing for (n-hexane + 1-pentanol, or 1-hexanol, or 1-heptanol) at T = 298.15 K, J. Chem. Thermodyn. 32 (2000) 923–930, https://doi.org/10.1006/jcht.2000.0661.
[25] M.A. Rivas, S.M. Pereira, T.P. Iglesias, Relative permittivity of the mixtures (dimethyl or diethyl carbonate) + n-nonane from T=288.15 K to T=308.15 K, J. Chem. Thermodyn. 34 (2002) 1897–1907, https://doi.org/10.1016/S0021-9614(02)00260-4.
[26] S.M. Pereira, T.P. Iglesias, J.L. Legido, M.A. Rivas, J.N. Real, Relative permittivity increments for $xCH_3OH + (1–x)CH_3OCH_2(CH_2OCH_2)_3CH_2OCH_3$ from T = 283.15 K to T = 323.15 K, J. Chem. Thermodyn. 33 (2001) 433–440, https://doi.org/10.1006/jcht.2000.0746.
[27] D.R. Lide (Ed.), Handbook of Chemistry and Physics, 90th ed., CRC Press, Boca Raton, Fl, 2010.
[28] G.J. Hill, The precise determination of the dielectric properties of alumina, IEEE Trans. Instrum. Meas. 23 (1974) 443–446, https://doi.org/10.1109/TIM.1974.4314331.
[29] www.accuratus.com, (accessed 2 January 2020).
[30] S. Lee, S.U.S. Choi, S. Li, J.A. Eastman, Measuring thermal conductivity of fluids containing oxide nanoparticles, J. Heat Transfer 121 (2) (1999) 280–289, https://doi.org/10.1115/1.2825978.
[31] T.P. Iglesias, J.C.R. Reis, L. Fariña-Busto, On the definition of the excess permittivity of a fluid mixture. II, J. Chem. Thermodyn. 40 (2008) 1475–1476, https://doi.org/10.1016/j.jct.2008.04.011.
[32] J.C.R. Reis, T.P. Iglesias, G. Douhéret, M.I. Davis, The permittivity of thermodynamically ideal liquid mixtures and the excess relative permittivity of binary dielectrics, Phys. Chem. Chem. Phys. 11 (2009) 3977–3986, https://doi.org/10.1039/B820613A.
[33] M.A. Rivas, T.P. Iglesias, S.M. Pereira, N. Banerji, On the permittivity and density measurements of binary systems of triglyme + (n-nonane or n-dodecane) at various temperatures, J. Chem. Thermodyn. 37 (2005) 61–71, https://doi.org/10.1016/j.jct.2004.08.003.
[34] M.A. Rivas, A.H. Buep, T.P. Iglesias, Study of the binary mixtures of monoglyme + (hexane, cyclohexane, octane, dodecane) by ECM-average and PFP models, J. Chem. Thermodyn. 89 (2015) 69–78, https://doi.org/10.1016/j.jct.2015.05.006.
[35] M.F. Coelho, M.A. Rivas, G. Vilão, E.M. Nogueira, T.P. Iglesias, Permittivity and electrical conductivity of copper oxide nanofluid (12 nm) in water at different temperatures, J. Chem. Thermodyn. 132 (2019) 164–173, https://doi.org/10.1016/j.jct.2018.12.025.
[36] H. Looyenga, Dielectric constants of heterogeneous mixtures, Physica 31 (1965) 401–406, https://doi.org/10.1016/0031-8914(65)90045-5.
[37] J.C. Maxwell, Electricity and Magnetism, Clarendon Press, Oxford, UK, 1873.
[38] C.W. Nan, Z. Shi, Y. Lin, A simple model for thermal conductivity of carbon nanotube-based composites, Chem. Phys. Lett. 375 (2003) 666–669. https://doi:10.1016/S0009-2614(03)00956-4.

JCT D-20-00298